Supporting Information for "Global structure of magnetotail reconnection revealed by mining space magnetometer data"

G. K. Stephens[1], M. I. Sitnov[1], R. S. Weigel[2], D. L. Turner[1], N. A. Tsyganenko[3], A. J. Rogers[4], K. Genestreti[5], and J. A. Slavin[6]

[1]The Johns Hopkins University Applied Physics Laboratory, Laurel, MD 20723, USA

[2]George Mason University, Fairfax, VA 22030, USA

[3]Saint-Petersburg State University, Saint-Petersburg, Russia

[4]University of New Hampshire, Durham, NH, USA

[5]Space Science and Engineering, Southwest Research Institute, Durham, NH, USA

[6]Department of Climate and Space Sciences and Engineering, University of Michigan, Ann Arbor, MI, USA

Contents of this file

Additional Supporting Information (Files uploaded separately)

Introduction

This study involves data-mining based empirical reconstructions of 26 ion diffusion region (IDR) events observed by the Magnetospheric Multiscale (MMS) Mission using a multi-decade and multi-spacecraft archive of magnetometer data. The main article

describes the archive, but here a figure (Figure S1) is provided to show the spatial distribution of the records contained in the archive. The main article also presents figures showing the equatorial magnetic field landscape (Figure 2) and the meridional current and magnetic field distributions (Figure 3) for 4 of the 26 IDR events. Here, complementary figures are included for the remaining 22 events: Figures S2-S7 show equatorial B_z distributions in the format of Figure 2. Figures S8-S13 show meridional currents and magnetic field lines in the meridional planes in the format of Figure 3, which contain the corresponding IDRs marked in Figures S2-S7.

Figure S14 provides the 3D global picture of the magnetosphere for event Y in a format similar to Figure 1, now with additional field lines near magnetic nulls determined as intersections of the neutral plane $B_x = 0$, $B_z = 0$ contour and the surface $B_y = 0$.

Movie S1. A movie showing the evolution of the equatorial magnetic field for the 26 July 2017 substorm containing event H. This movie complements Figure 6 from the main article. (a and b) Geomagnetic indices and solar wind parameters in a similar format as described in Figure 2. (c) Equatorial magnetic field, B_z, in a similar format as Figure 2. The location of MMS is indicated by the green dot.

References

Li, T., Priest, E., & Guo, R. (2021). Three-dimensional magnetic reconnection in astrophysical plasmas. *Proc. Royal Soc. A*, *477*(2249), 10.1098/rspa.2020.0949. doi: https://doi.org/10.1098/rspa.2020.0949

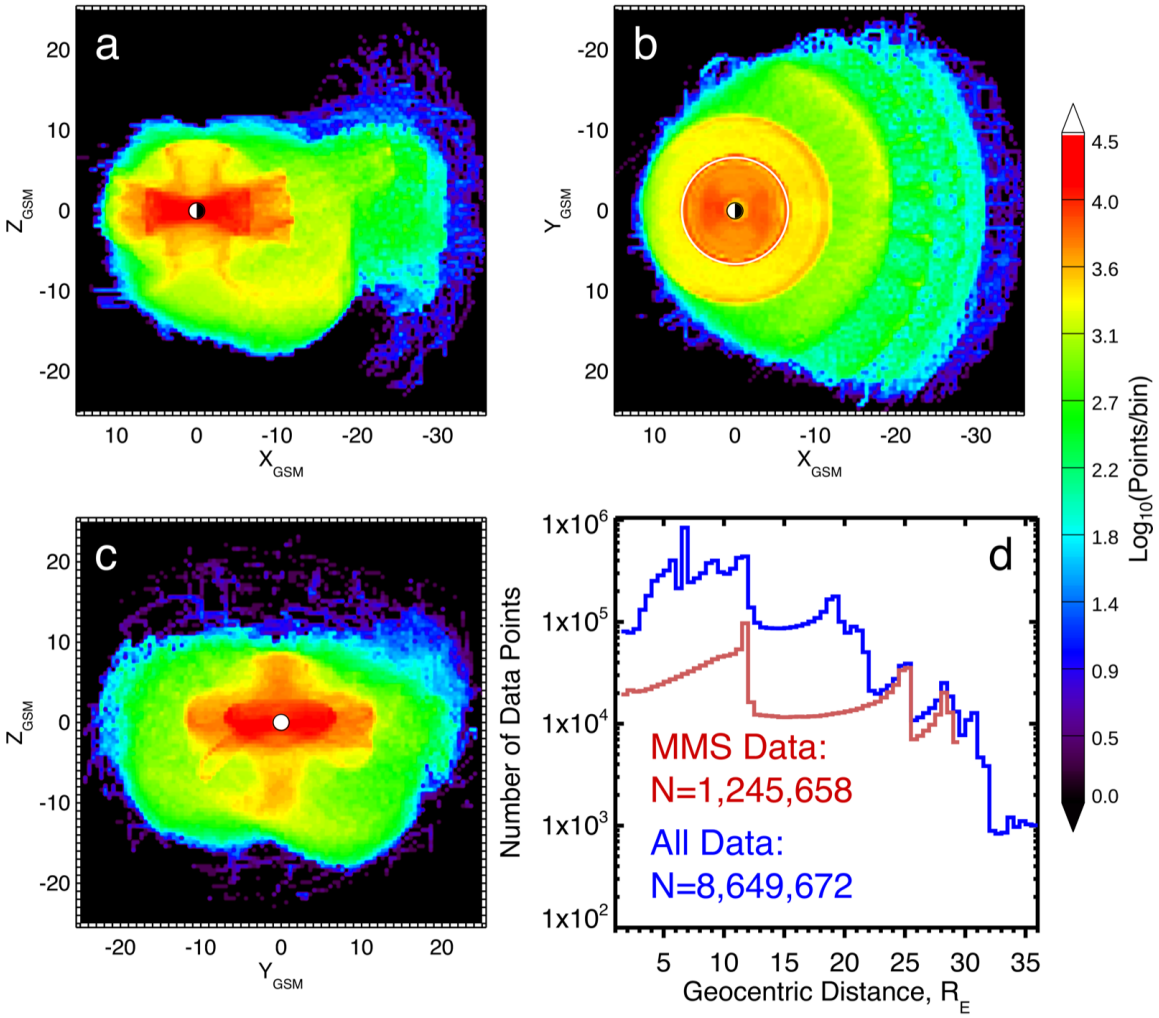

Figure S1. Distribution of data records in the archive of space magnetometer data. (a, b, and c) A 2D histogram displaying the spatial distribution a data records projected into the (a) meridional, (b) equatorial, and (c) Y-Z planes in the GSM coordinate system. The color indicates the number of points in each $0.5R_E$ by $0.5R_E$ bin using a logarithmic scale, with red/purple corresponding to regions with a dense/sparse density of data records. Black regions contain zero data records. (d) A 1D histogram showing the number of data records in $0.5R_E$ radial bins (spherical shells) using a logarithmic scale with the total archive in blue and just the MMS dataset in red.

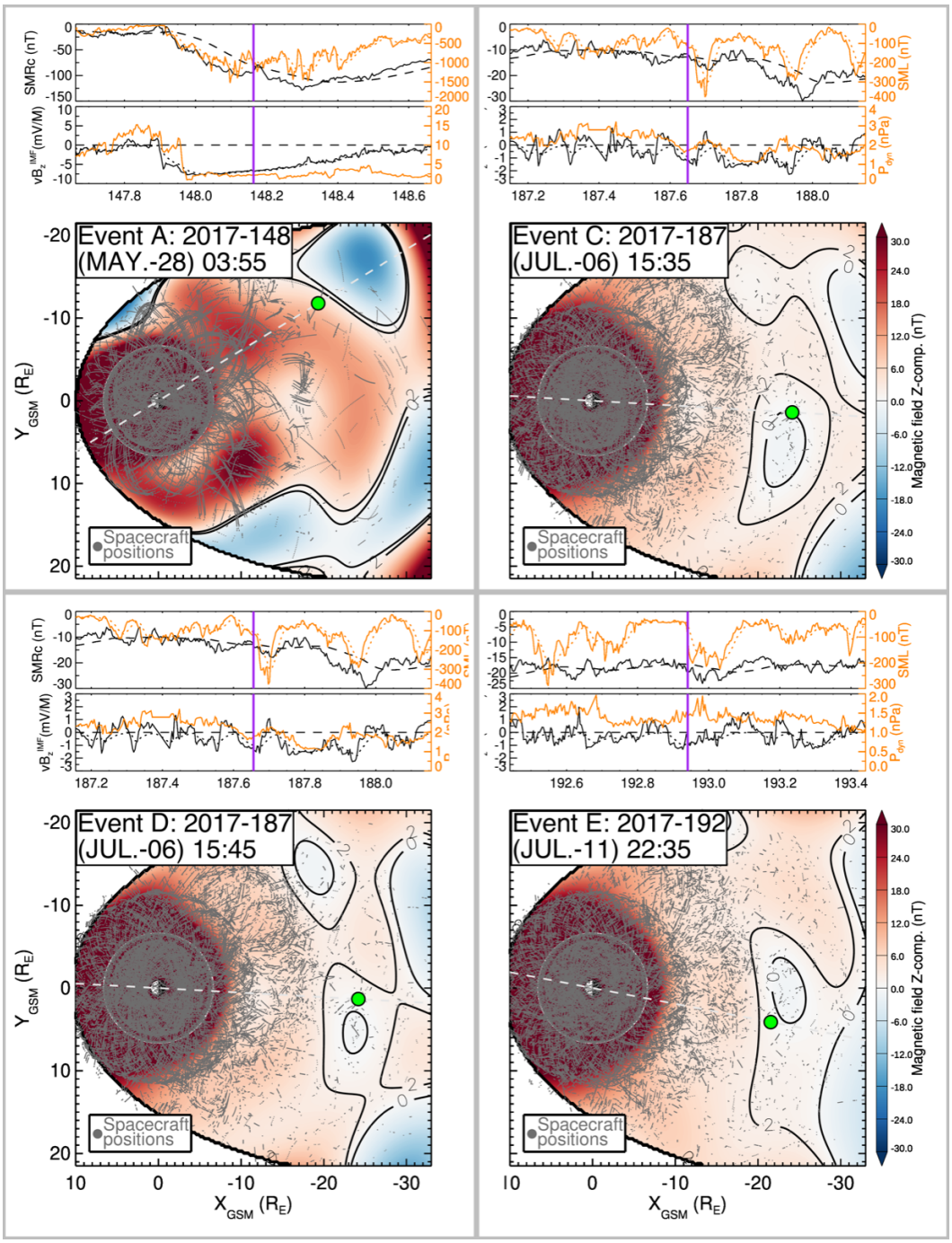

Figure S2. Ion diffusion regions and the equatorial magnetic field landscape. The format is similar to Fig. 2 except for a different group of IDR events: A, C, D, and E, with the MMS IDR locations marked by green dots. These four events are considered "Hits" as the $B_z = 0$ contour is within $< 2R_E$ of the observed MMS IDR.

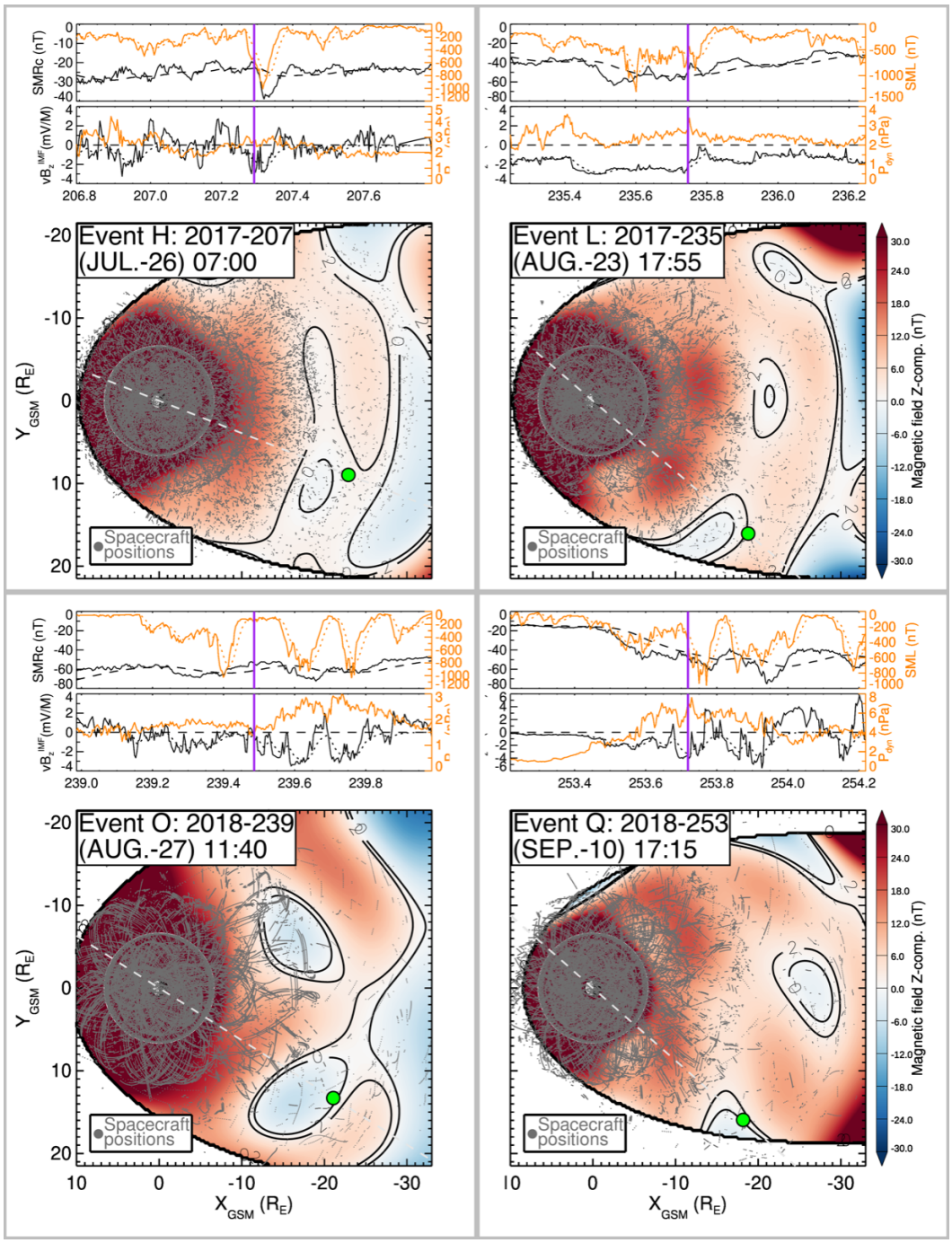

Figure S3. Ion diffusion regions and the equatorial magnetic field landscape. The format is similar to Fig. S2 except for a different group of IDR events: H, L, O, and Q, with the MMS IDR locations marked by green dots. These four events are considered "Hits" as the $B_z = 0$ contour is within $< 2R_E$ of the observed MMS IDR.

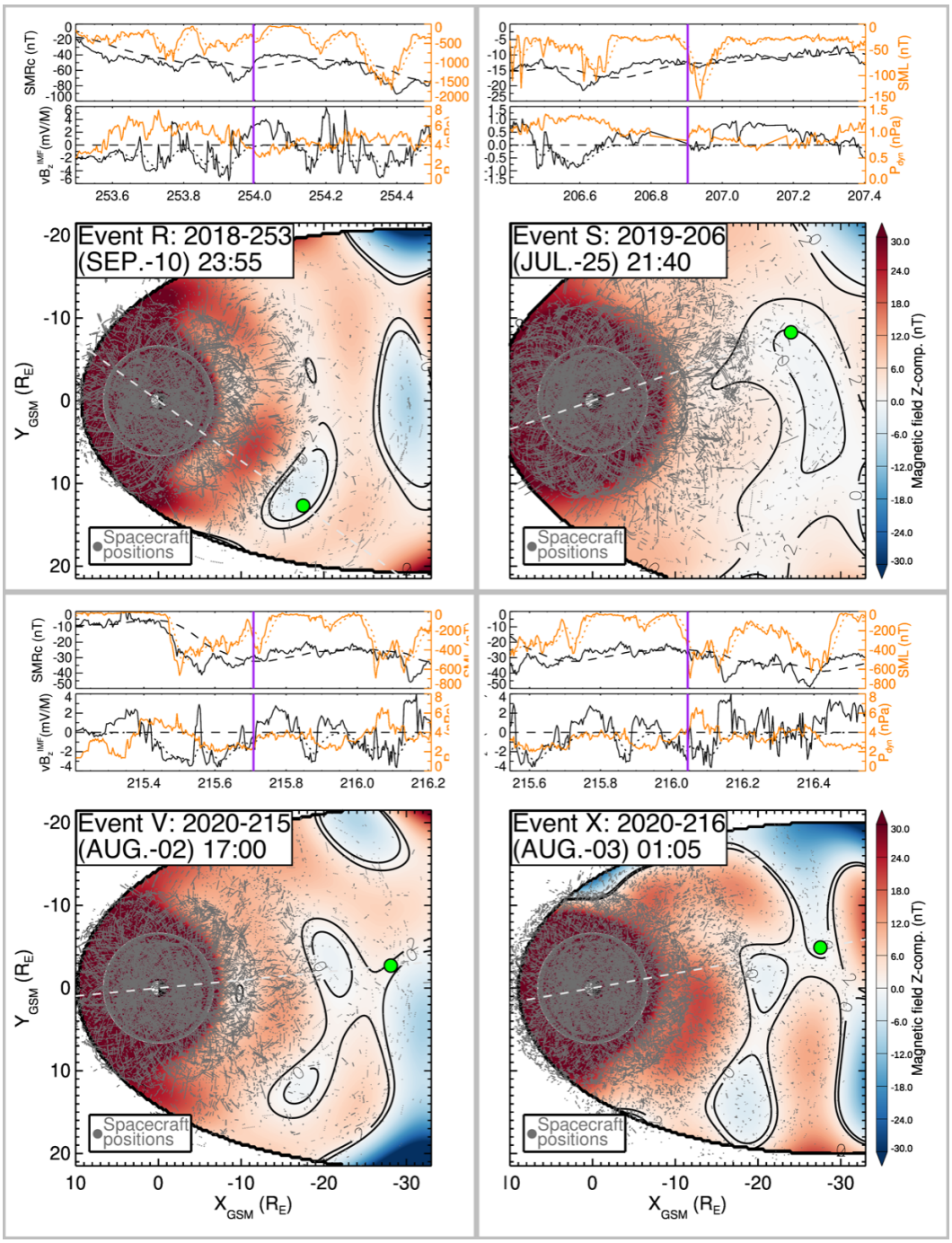

Figure S4. Ion diffusion regions and the equatorial magnetic field landscape. The format is similar to Fig. S2 except for a different group of IDR events: R, S, V, and X, with the MMS IDR locations marked by green dots. These four events are considered "Hits" as the $B_z = 0$ contour is within $< 2R_E$ of the observed MMS IDR.

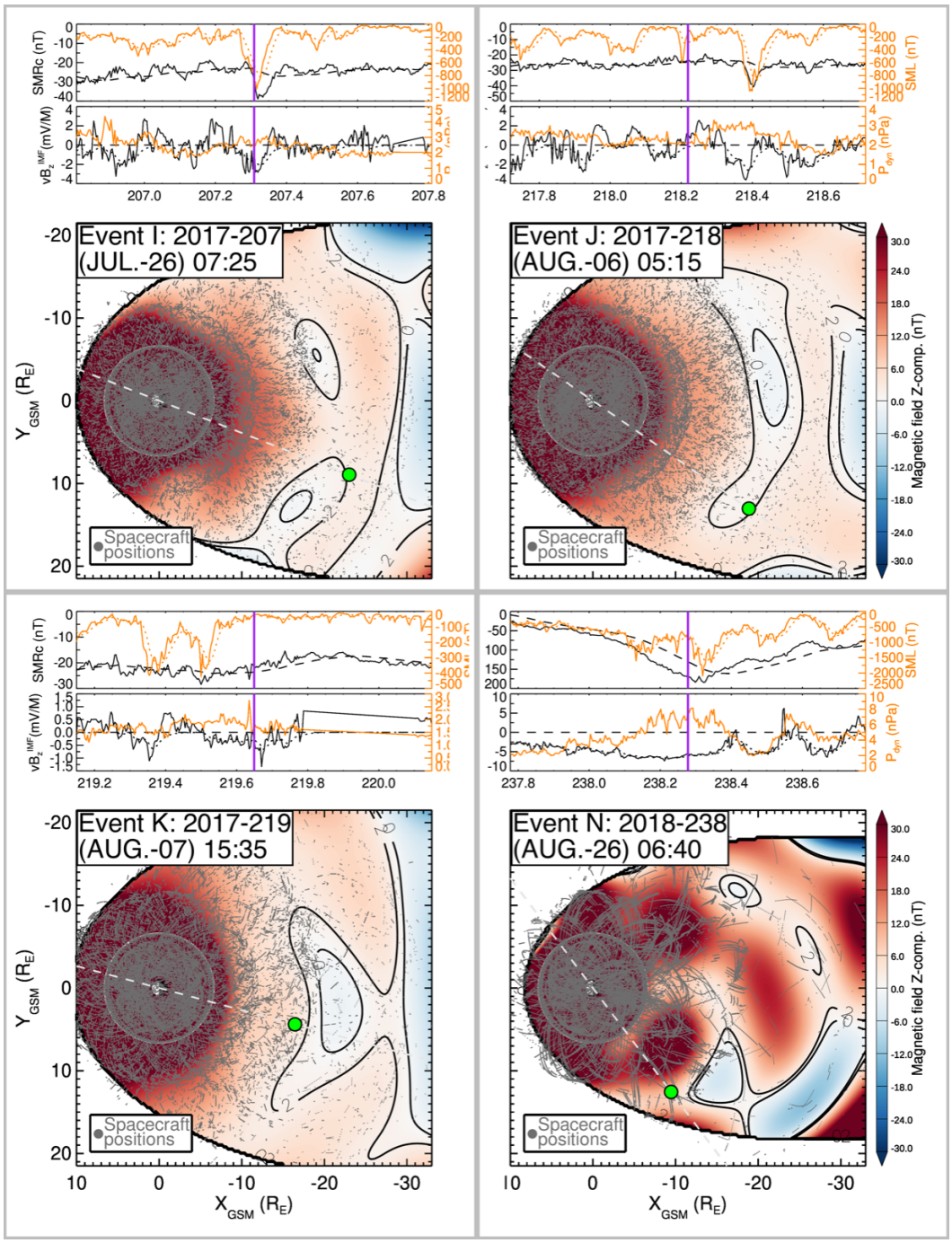

Figure S5. Ion diffusion regions and the equatorial magnetic field landscape. The format is similar to Fig. S2 except for a different group of IDR events: I, J, K, and N, with the MMS IDR locations marked by green dots. These four events are considered "Near Hits" as the $B_z = 2$ nT contour is within $< 2.2R_E$ of the observed MMS IDR.

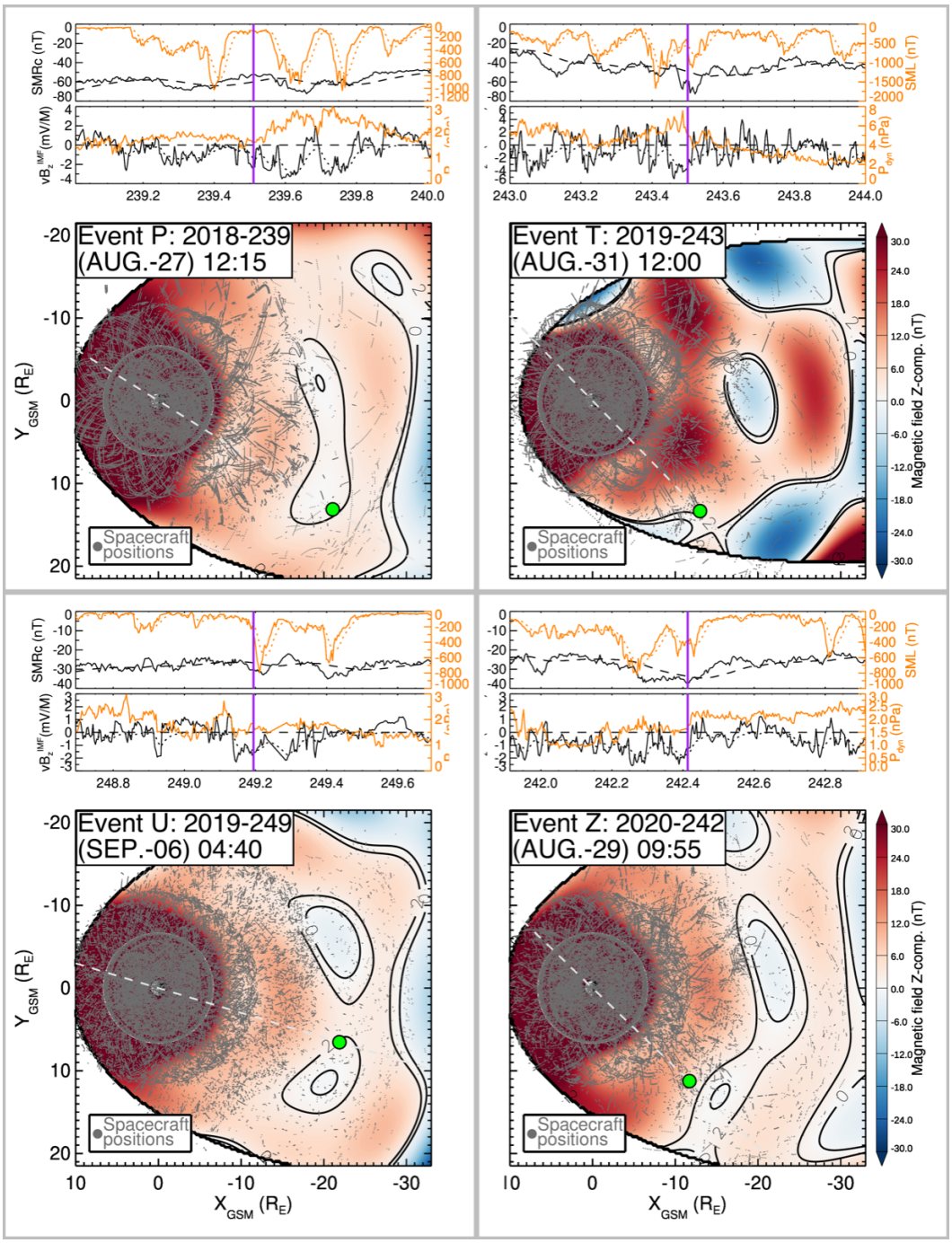

Figure S6. Ion diffusion regions and the equatorial magnetic field landscape. The format is similar to Fig. S2 except for a different group of IDR events: P, T, U, and Z, with the MMS IDR locations marked by green dots. These four events are considered "Near Hits" as the $B_z = 2$ nT contour is within $< 2.2R_E$ of the observed MMS IDR.

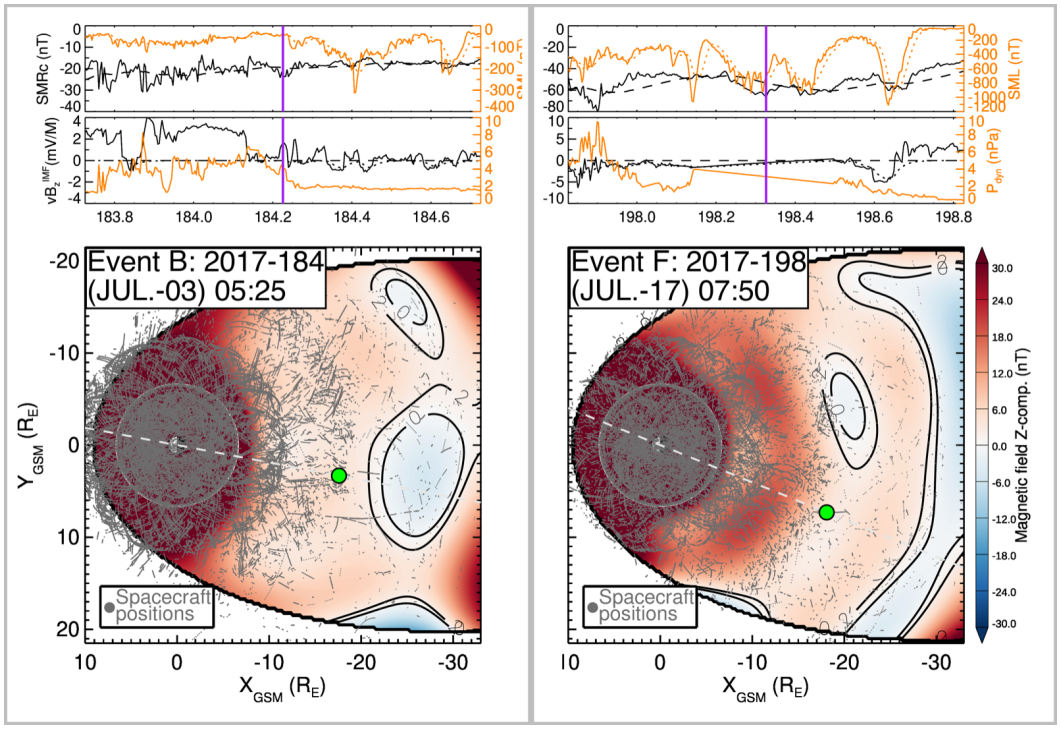

Figure S7. Ion diffusion regions and the equatorial magnetic field landscape. The format is similar to Fig. S2 except for a different group of IDR events B and F, with the MMS IDR locations marked by green dots. The contours $B_z = 0$ nT and $B_z = 2$ nT are not close to the observed MMS IDR locations.

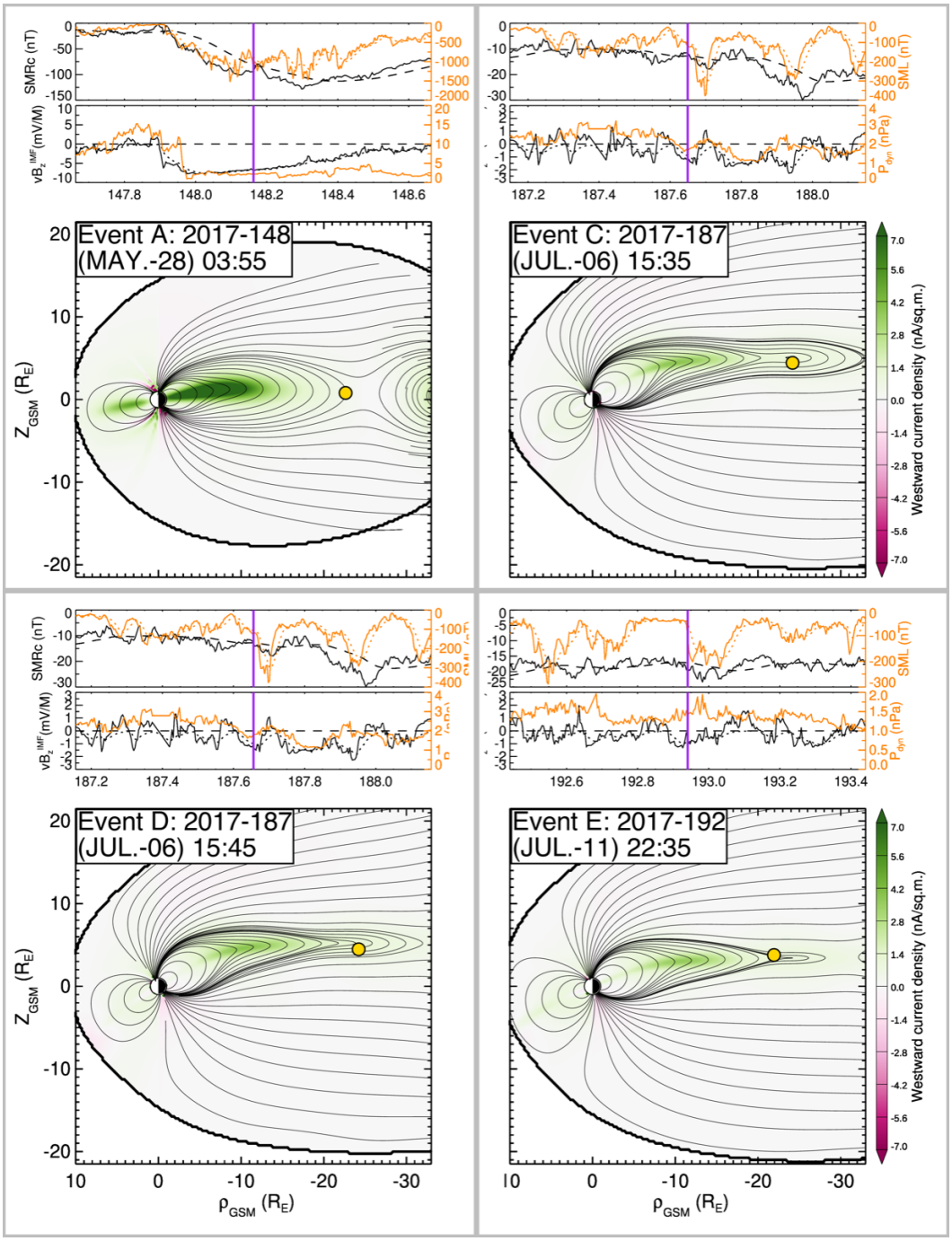

Figure S8. Ion diffusion regions against the meridional current and magnetic field distributions for events A, C, D, and E, with the MMS IDR locations marked by orange dots. The format is similar to Fig. 3.

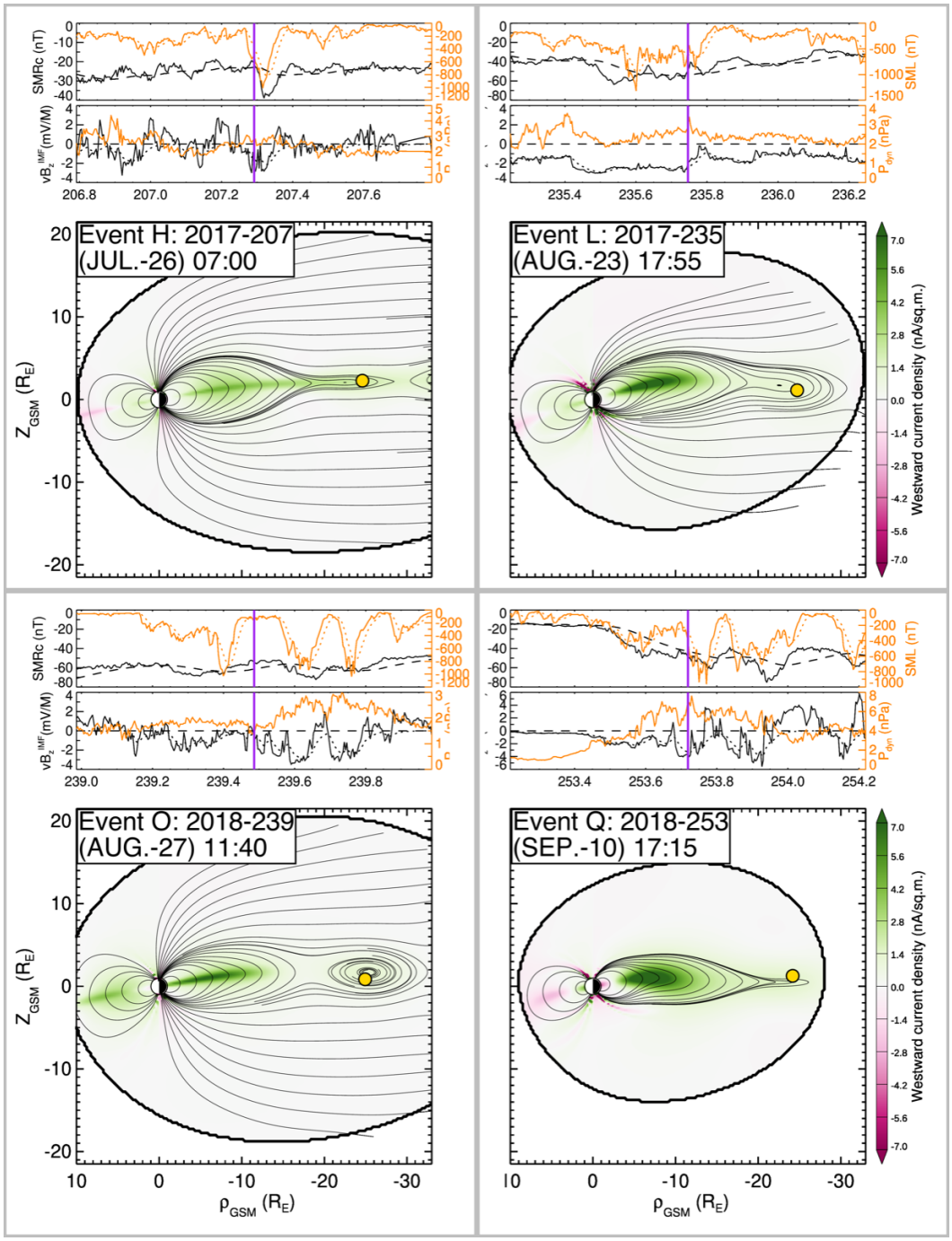

Figure S9. Ion diffusion regions against the meridional current and magnetic field distributions for events H, L, O, and Q, with the MMS IDR locations marked by orange dots. The format is similar to Fig. S8.

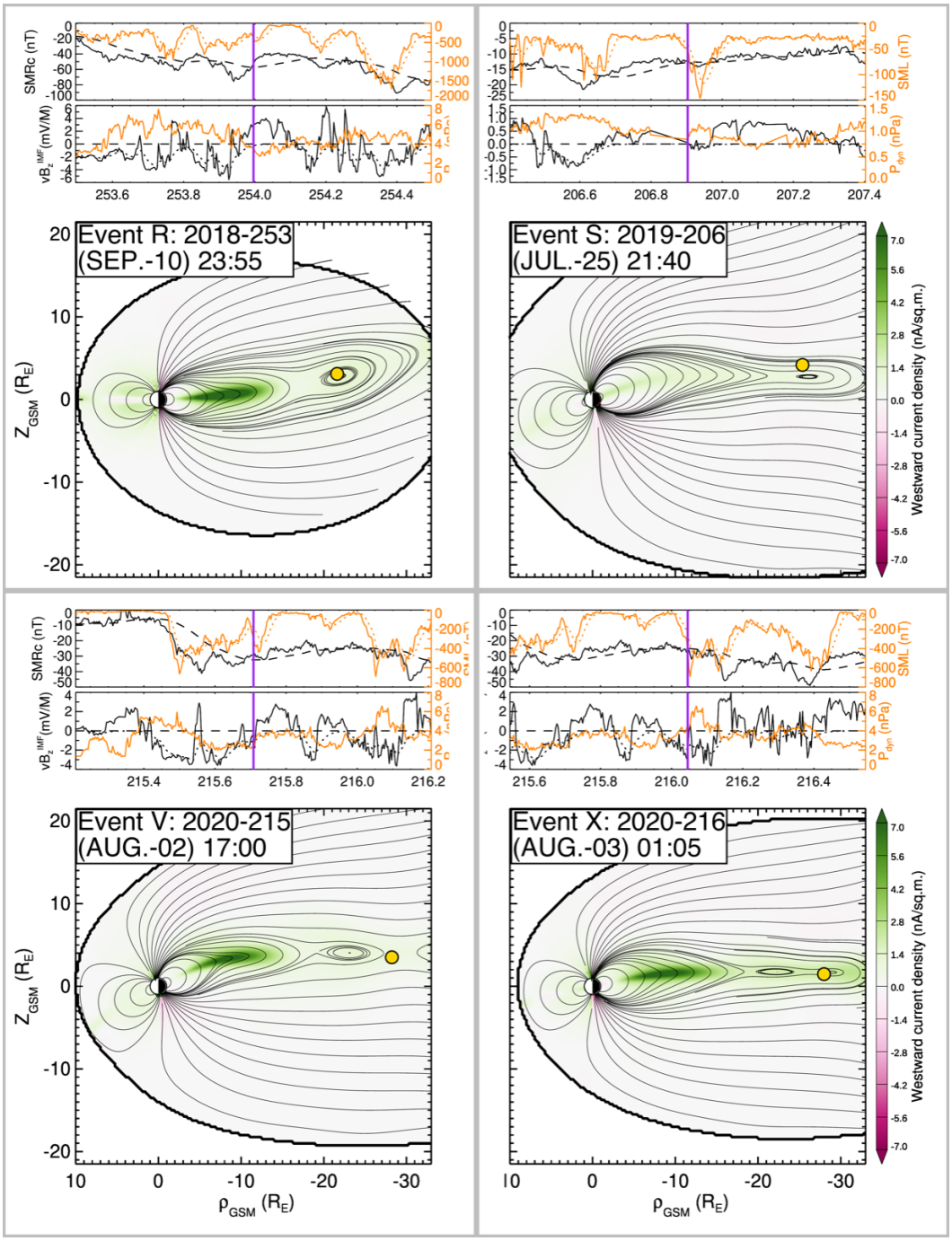

Figure S10. Ion diffusion regions against the meridional current and magnetic field distributions for events R, S, V, and X, with the MMS IDR locations marked by orange dots. The format is similar to Fig. S8.

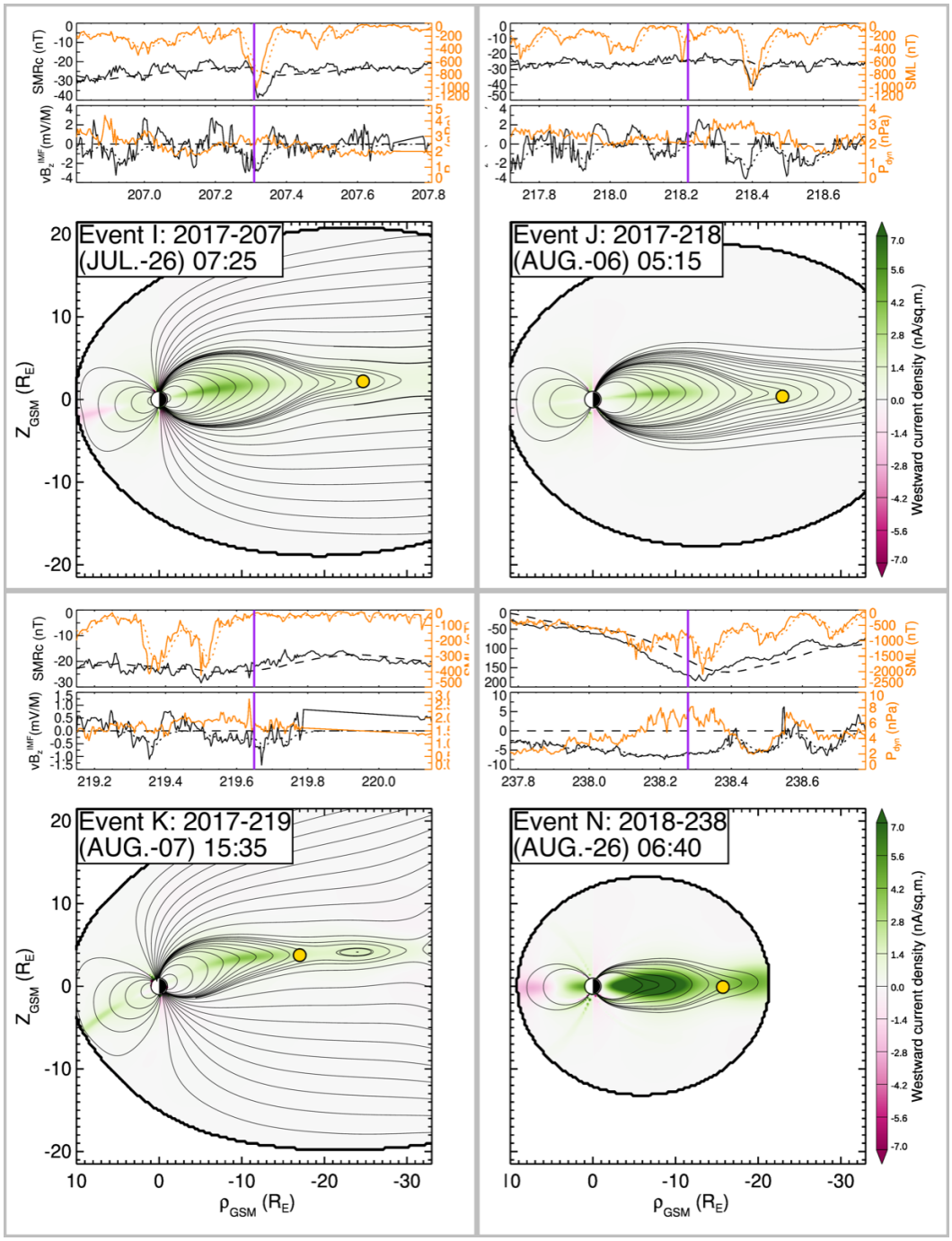

Figure S11. Ion diffusion regions against the meridional current and magnetic field distributions for events I, J, K, and N, with the MMS IDR locations marked by orange dots. The format is similar to Fig. S8.

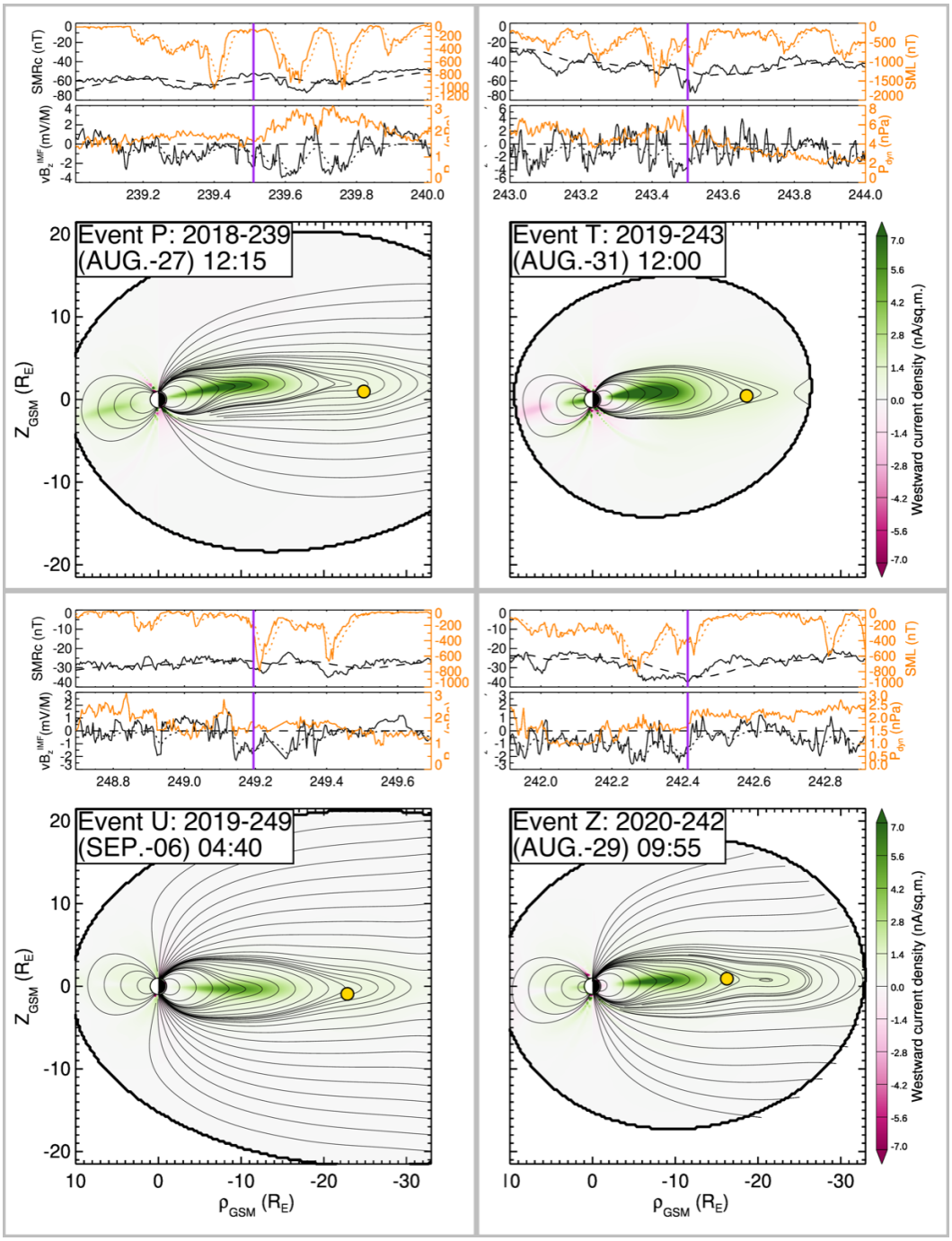

Figure S12. Ion diffusion regions against the meridional current and magnetic field distributions for events P, T, U, and Z, with the MMS IDR locations marked by orange dots. The format is similar to Fig. S8.

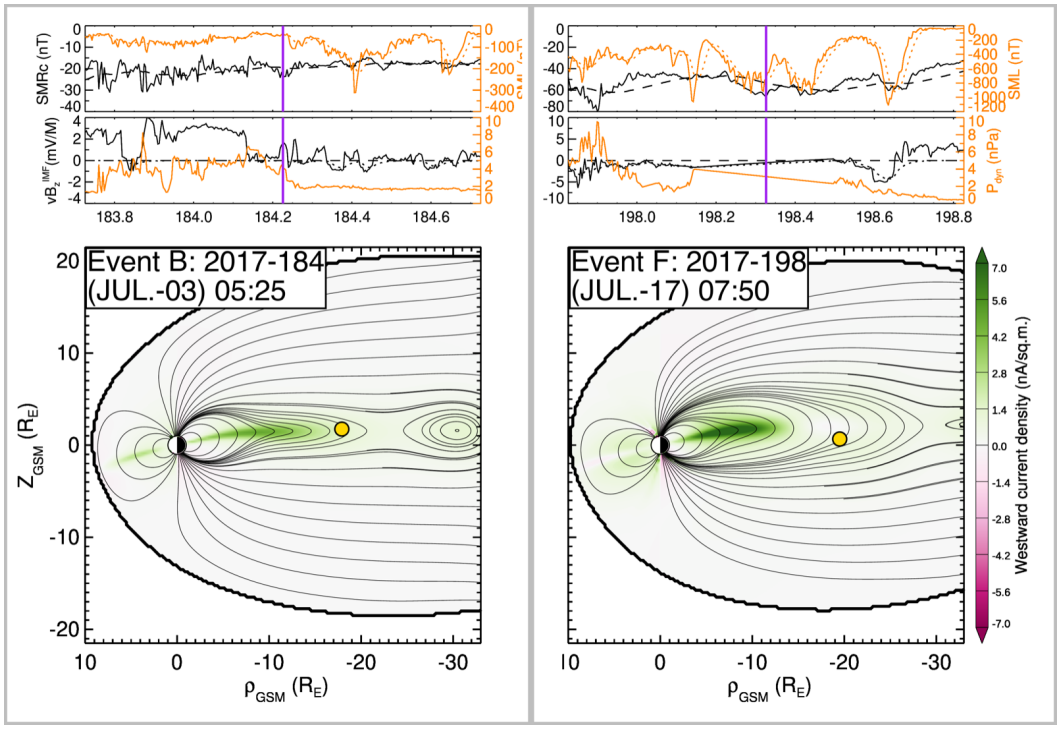

Figure S13. Ion diffusion regions against the meridional current and magnetic field distributions for events B and F, with the MMS IDR locations marked by orange dots. The format is similar to Fig. S8.

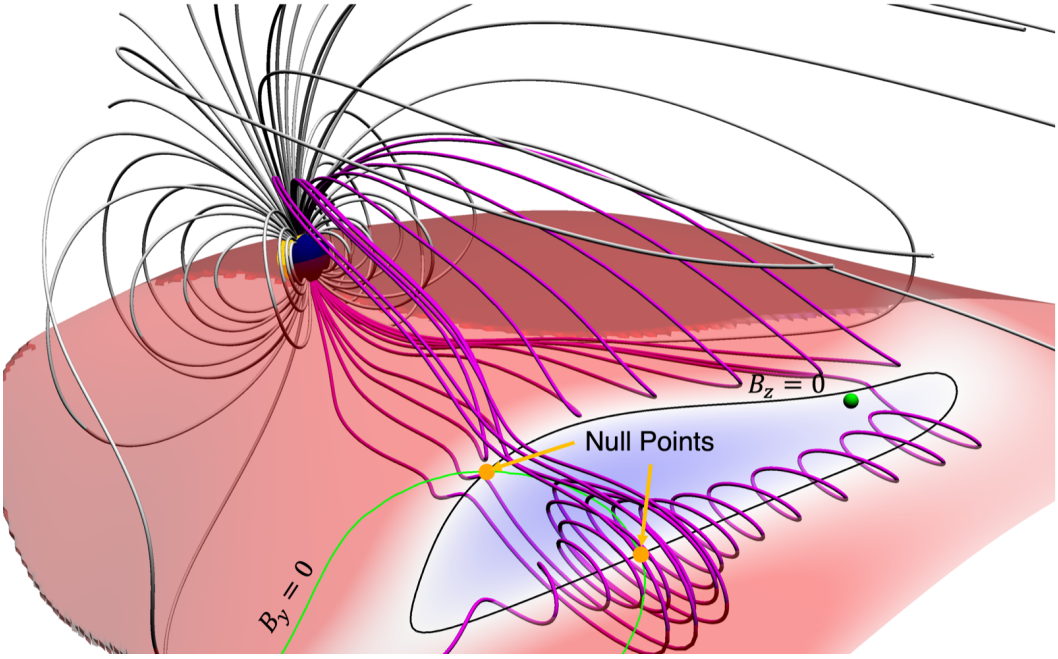

Figure S14. 3D global picture of the magnetosphere with more field lines near the expected magnetic nulls (orange tadpole marks), which are defined as intersections of the surface $B_y = 0$ with the equatorial $B_z = 0$ loop shown in Fig. 1 (event Y). According to the null nomenclature (Li et al., 2021), the near-Earth and more distant null areas correspond to radial and spiral nulls.